Eur Biophys J (2002) 31: 198–206
DOI 10.1007/s00249-002-0206-6

ARTICLE

Graham R. Smith · Mark S.P. Sansom

Free energy of a potassium ion in a model of the channel formed by an amphipathic leucine-serine peptide

Received: 8 August 2001 / Revised: 19 December 2001 / Accepted: 19 December 2001 / Published online: 19 February 2002

Abstract We use molecular dynamics simulations to investigate the position-dependent free energy of a potassium ion in a model of an ion channel formed by the synthetic amphipathic leucine-serine peptide, LS3. The channel model is a parallel bundle of six LS3 helices around which are packed 146 methane-like spheres in order to mimic a membrane. At either end of and within the channel are 1051 water molecules, plus four ions (two potassium and two chloride). The free energy of a potassium ion in the channel was estimated using the weighted histogram analysis (WHAM) method. This is the first time to our knowledge that such a calculation has been carried out as a function of the position of an ion in three dimensions within a channel. The results indicate that for this channel, which is lined by hydrophilic serine sidechains, there is a relatively weak dependence of the free energy on the axial/off-axial position of the ion. There are some off-axis local minima, especially in the C-terminal half of the channel. Using the free energy results, a single channel current-voltage curve was estimated using a one-dimensional Nernst-Planck equation. Although reasonable agreement with experiment is achieved for K^+ ions flowing from the N-terminal to the C-terminal mouth, in the opposite direction the current is underestimated. This underestimation may be a consequence of under-sampling of the conformational dynamics of the channel. We suggest that our simulations may have captured, for example, a sub-conductance level (i.e. an incompletely open state) of the LS3 channel.

Keywords Leucine-serine peptide · Ion channels · Potassium ion · Molecular dynamics · Simulations

G.R. Smith[1] · M.S.P. Sansom (✉)
Laboratory of Molecular Biophysics,
Department of Biochemistry, Rex Richards Building,
University of Oxford, South Parks Road,
Oxford OX1 3QU, UK
E-mail: mark@biop.ox.ac.uk
Tel.: +44-1865-275371
Fax: +44-1865-275182

Present address:
[1]Biomolecular Modelling Laboratory,
Imperial Cancer Research Fund,
44 Lincoln's Inn Fields, London WC2A 3PX, UK

Introduction

Despite the wealth of data on the electrophysiology (Hille 1992) of ion channels and continuing advances in our knowledge of their structures (Chang et al. 1998; Doyle et al. 1998; Ketchem et al. 1993; Miyazawa et al. 1999), the permeation process is still imperfectly understood because of the difficulty in quantitatively predicting the properties of the channel, even in cases where the structure is known (Eisenberg 1999; Partenskii and Jordan 1992; Roux 1999; Roux et al. 2000; Tieleman et al. 2001). Here, we focus on an aspect of the conductance-prediction problem. An important input to this is the position-dependent free energy of an ion in the channel under conditions of electrochemical equilibrium (Åqvist and Luzhkov 2000; Bernèche and Roux 2001; Hao et al. 1997; Roux 1996), and we are developing methods to estimate this free energy using computer simulation; we test these methods here by determining the free energy of a potassium ion in a model of the channel formed by a synthetic peptide. Even once this free-energy profile is calculated, using it in the prediction of conductance is a difficult task, as no exact non-equilibrium theory of ion channels exists. Nevertheless, approximate descriptions like the Nernst-Planck equation are expected to have reasonable validity. They have already been used with some success (Dieckmann et al. 1999) in cases where the effective potential in the channel is estimated by continuum electrostatic theory (Adcock et al. 1998, 2000; Kienker et al. 1994; Woolley et al. 1997).

The peptide that we have chosen to study is LS3, an artificial channel-forming peptide consisting of alternating blocks of leucine and serine amino acid residues

(Åkerfeldt et al. 1993; Lear et al. 1988). LS3 has been the subject of extensive studies by electrophysiology (Kienker et al. 1994; Kienker and Lear 1995; Lear et al. 1988) and computer simulation, both in this group (Mitton and Sansom 1996; Randa et al. 1999) and elsewhere (Chen et al. 1997; Dieckmann et al. 1999; Kienker et al. 1994; Zhong et al. 1998), so that we already have estimates of other parameters relevant to ion permeation, such as the ionic diffusion coefficient in the channel (Smith and Sansom 1998, 1999). As mentioned before, there have also been calculations of conductance based on a continuum electrostatics approach to a series of models, including one from a molecular dynamics (MD) model (Dieckmann et al. 1999). These considerations make LS3 a good test-bed for the free energy calculations.

Methods

Simulations

The channel model consists of a parallel bundle of six LS3 helices; the sequence of each helix is Ac-$(LSSLLSL)_3$-NH_2. The starting helix bundle was extracted from the time-slice at ca. 2.3 ns of a simulation (GMX) of an LS3 hexamer inserted into a fully hydrated POPC lipid bilayer (Randa et al. 1999). The protein was thus well relaxed in a bilayer environment. The configuration used was taken from the 2–4 ns interval of the full bilayer simulation in which the pore-lining atoms of the bundle had the greatest symmetry. In the simulation system used for the free energy calculations (CHM), no lipid molecules are included, but the channel is packed around along its entire length by 146 Lennard-Jones spheres, with parameters appropriate for an extended-atom representation of methane (Jorgensen et al. 1989). The system is solvated with 1051 modified TIP3P water molecules (the waters in the channel, of which there are about 100, being kept from the full bilayer simulation and the rest added from a pre-equilibrated rectangular box), and four ions are also introduced, two potassium and two chloride. As there are no ionizable residues in the LS3 peptide, the system is electrically neutral, and the ionic concentration is 0.105 M, a value typical of those used in experimental studies. The protein is modelled using the Charmm parameter 19 set, which is an extended atom parameter set (i.e. aromatic and aliphatic hydrogen atoms are not represented explicitly). The simulation system (Fig. 1) thus consists of a box of dimensions 31.1×31.1×62.2 Å, with periodic boundary conditions, containing 4419 atoms of which 1116 are protein atoms. The axis of the channel is along the z-axis of the simulation system, with its centre near the coordinate origin, and the channel (and surrounding methane spheres) extending from about $z = -18$ Å to $+17$ Å. This system was equilibrated in its new configuration for 200 ps.

During this simulation and the subsequent ones from which the free energy is to be estimated, the Cα atoms of the protein and the methane atoms are restrained to remain close to their original starting positions by positional restraints having a force constant of 0.1 kcal mol^{-1} $Å^{-2}$ (arrived at by a method described at the start of the results section). No restraints are applied to the water. The chloride ions and one of the potassium ions were placed in the water caps, where they are free to move, and the other potassium is restrained to a variety of positions in the channel using Charmm's MMFP restraints, as will be described in more detail later. The simulation protocol for each position of the potassium is as follows. One of the K^+ ions (always the same one) is exchanged with the water molecule nearest the desired position of the ion in the channel, and the system is minimized with the ion fixed over 3000 steps using the adopted-basis Newton-Raphson method. The system is then heated to 300 K over 6000 MD steps by rescaling velocities, still with the K^+ ion fixed. The system is then minimized again, and then re-heated, now with the ion no longer fixed but restrained with MMFP restraints. Finally 20,000 steps of equilibration and 100,000 steps of production are performed, with the MMFP restraints maintained throughout on the K^+ ion. The MD step size is 1 fs, so each production trajectory is 100 ps long, with SHAKE used on bonds to hydrogen. The ions in the caps may move approximately 5 Å in this time. Coordinates are saved every 0.1 ps. The equilibration and production runs are performed at a constant temperature of 300 K with the Nosé-Hoover thermostat. Long-range electrostatic interactions are calculated throughout using the particle-mesh Ewald method, with the short-range interactions, calculated in real space, cut off at 9 Å. However, the periodic replication of the system (set up with the Charmm IMAGE command) is carried out only for the water and ions, not for the protein, so that the simulation system corresponds more closely to a single channel at infinite dilution than to a very concentrated protein system. Because of this replication, the effect of the apparent asymmetry of the system (a potassium and a chloride in one water cap and a chloride alone in the other) will not be severe; indeed, the potassium ion was quite near (1–5 Å) to the periodic boundary in z and was thus effectively approximately equidistant from the two mouths of the channel.

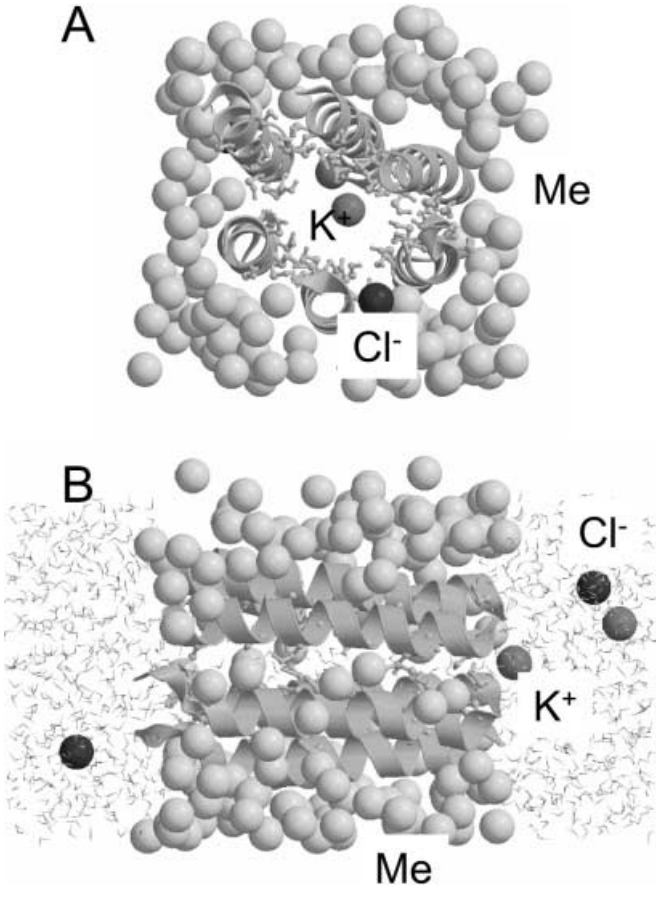

Fig. 1 The simulation system: **A** view perpendicular to the channel (z) axis; **B** view down the channel axis. The protein is shown in *ribbons* representation, with the side chains of serine residues in *balls-and-sticks* format. The methane spheres (Me) are shown as van der Waals spheres (*light grey*), as are potassium ions (K^+; *mid grey*) and chloride ions (Cl^-; *dark grey*). In **B** the water molecules are shown in *bonds* format. The figure was produced using Molscript (Kraulis 1991) and Raster3D (Merritt and Bacon 1997)

A total of 250 different positions of the K^+ ion have been investigated, so the total production simulation time is 30 ns. In all of these runs, the starting configuration of all atoms (except the K^+ ion and the water it is exchanged with) is the same, i.e. the $(n+1)$th simulation is not started from the final configuration of the nth. The setting-up of each run was done with perl scripts and the MD runs carried out using Charmm version 25b2 on Silicon Graphics Origin 2000 and DEC Alpha-AXP ev56 servers.

Free energy

The free energy profile is calculated by an umbrella sampling technique (Torrie and Valleau 1977). If the equilibrium probability (in the canonical ensemble) of an ion to be found at a point $\boldsymbol{r}=(x,y,z)$ is $P(\boldsymbol{r})\mathrm{d}^3r$, then the position-dependent free energy of the ion at that point is $F(\boldsymbol{r})$, where:

$$F(\mathbf{r}) = -RT\ln(P(\mathbf{r})) \tag{1}$$

However, $P(\boldsymbol{r})$ cannot easily be measured directly by simulation, because the time to explore the whole channel would be prohibitively long. This would be true even if $P(\boldsymbol{r})$ were fairly uniform; the problem is exacerbated by the presence of free energy barriers that constitute local minima in $P(\boldsymbol{r})$ [corresponding to maxima in $F(\boldsymbol{r})$]. The rate k of crossing such barriers generally decreases exponentially with the barrier height [the activation free energy $G=F(\boldsymbol{r})$], according to the Arrhenius law:

$$k = v\exp(-G^{\ddagger}/kT) \tag{2}$$

One solution is to apply additional, artificial potentials to enable a more controlled exploration of the volume of the channel by the ion; the effect of these potentials can then be corrected for and $P(\boldsymbol{r})$ in the unperturbed system recovered. The additional potentials are often chosen to cancel the free energy barriers and permit a more extensive exploration of the desired volume, but here the approach taken is to confine the K^+ ion in a series of overlapping *cubic* boxes generated with Charmm's MMFP restraints. The side length of each box is chosen to be $\Delta x_0 = 3.0$ Å and it overlaps by 1.0 Å with its neighbours on each side. The depth of the confining potential well is $V_0 = 10$ kcal mol^{-1} in each of the x, y and z directions, and it rises over a typical distance of $a = 0.1$ Å; that is to say that the restraining potential is:

$$E_{\mathrm{MMFP}} = E_{\mathrm{R}}(x,x_0)+E_{\mathrm{R}}(y,y_0)+E_{\mathrm{R}}(z,z_0) \tag{3}$$

where:

$$\begin{aligned} &E_R(x,x_0;\Delta x_0,a) \\ &\quad = -V_0[1-(1/2)\exp(-(|x-x_0|-\Delta x_0)/a)] \quad \text{if } |x-x_0|>\Delta x_0 \\ &\quad = -(V_0/2)\exp(-(|x-x_0|-\Delta x_0)/a) \qquad \text{otherwise} \end{aligned} \tag{4}$$

x_0 varies between each box; the other parameters V_0, Δx_0 and a could also vary between boxes, though they were kept constant here. For each simulation, the probability density of the ion's position, $P'(\boldsymbol{r})$ (the $'$ indicating the ensemble perturbed with E_{MMFP}) can be estimated from the histograms of position (clearly, information is only obtained for $\boldsymbol{r}$ within the box), and then the unperturbed $P(\boldsymbol{r})$ (again within the box) can be estimated by using the normalization of each $P(\boldsymbol{r})$ and:

$$P(r) \approx P'(\mathbf{r})\exp(E_{\mathrm{MMFP}}(\mathbf{r})/RT) \tag{5}$$

This set of $P(\boldsymbol{r})$ values can then be combined to obtain a single $P(\boldsymbol{r})$ covering the entire channel by using the fact that P must be continuous and single-valued in the regions where adjacent simulation boxes overlap. In one dimension this overlapping is a simple operation; in a three-dimensional case like the present one, a solution is best found iteratively, using the weighted histogram analysis (WHAM) method (Kumar et al. 1992). Because of the sixfold symmetry of the system, the sampling has been performed only over a segment covering about 1/6 of the volume of the channel, which is then symmetrically replicated by repeated rotations about the z axis. $F(z)$ is obtained from:

$$F(z) = -RT\ln\left(\int P(r)\,\mathrm{d}x\,\mathrm{d}y\right) \tag{6}$$

In most cases, this means that $F(z)\approx\min(x,y)F(\boldsymbol{r})$. Similarly, one can define:

$$F(r) = F(r,z) = -RT\ln\left(\int P(r)\,\mathrm{d}\theta\right) \tag{7}$$

All other analysis was also performed using Charmm 25b2.

Channel conductance

A simple approximate method to estimate the current-voltage relation is then to use the Nernst-Planck equation (Hille 1992) in the form:

$$I = -qAD(z)[(c/RT)\mathrm{d}F(z)/\mathrm{d}z + \mathrm{d}c/\mathrm{d}z] \tag{8}$$

where A is the channel cross-sectional area, q is the ionic charge, D is its diffusion coefficient, and c is the ionic concentration (the latter may be also a function of z, but solving the equation requires only its values at the boundaries of the system, that is to say, in the bulk solutions on the two sides).

Results

As a preliminary, we investigate the effect that the size of the much smaller simulation system used here (CHM) has in comparison to the full bilayer simulation [GMX (Randa et al. 1999)] from which the initial coordinates were extracted. The fluctuation in pore radius calculated by the program HOLE (Smart et al. 1993) is compared for the two systems in Fig. 2. The configurations shown for the GMX simulation come from all 4 ns of the simulation, while for the CHM simulation they come from the 200 ps performed before inserting the ions. While differences are noticeable, the variation is reasonable, especially within the relatively short timescale of the Charmm simulations. At the N-terminus there is a single excursion in the CHM simulation to a very small radius; at the C-terminus the CHM simulation has a smaller degree of fluctuation and is appreciably narrower. The slight reduction in pore radius in the centre of the channel is also noteworthy. Preliminary tests were carried out on the helix bundle with three force constants: 0.01, 0.1 and 10 kcal mol^{-1} Å^{-2}. The 0.1 kcal mol^{-1} Å^{-2} force constant produced fluctuations in the channel diameter that were similar to those seen in the 4 ns MD simulation; the larger one produced fluctuations that were much smaller (results not shown), while the simulation with the 0.01 kcal mol^{-1} Å^{-2} force constant suffered a SHAKE error. Since it was thought better to perturb the natural motions of the channel as little as possible, and therefore to use weak restraints unless there was a compelling reason to do otherwise, the 0.1 kcal mol^{-1} Å^{-2} force constant was adopted.

It is important to be confident in the free energy results, that sampling within each of the MMFP "boxes" that the K^+ ion was confined in was adequate to give a

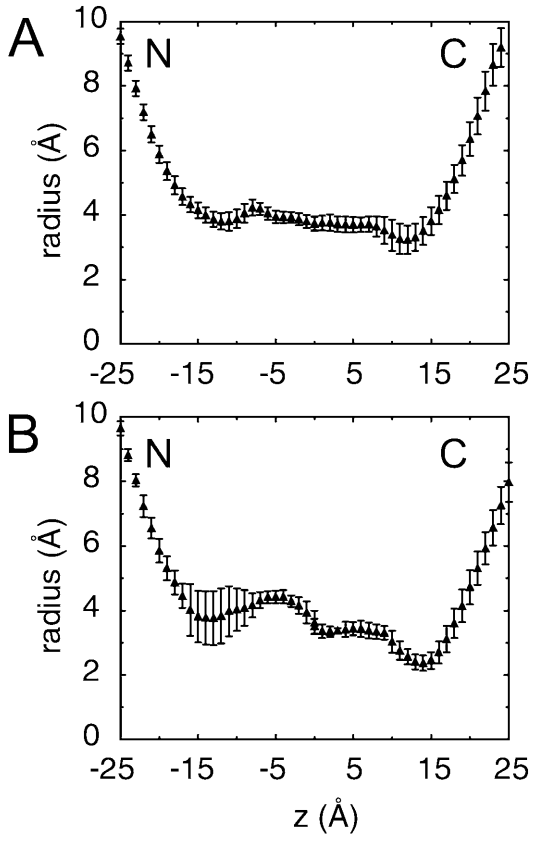

Fig. 2 The radius profile of the LS3 helix bundle, calculated by the program HOLE (Smart et al. 1993), for **A** the GROMACS simulation from which the initial configuration was taken (Randa et al. 1999), and **B** the Charmm simulation for which the free energy calculations were performed

good estimate of $P'(\boldsymbol{r})$. To quantify this, we have measured for each box the number of times the ion moves from one end of the box to the other (taking the "end" of the box to mean the first or final 1/5 of it). This was done for each of the three coordinate directions. It is found that, for the ion on the channel axis, there are 12 ± 4 such movements in each 100 ps trajectory, with no significant difference between x, y and z. At an off-axial position ($x = -3$ Å, $y = -3$ Å), and considering only those z-positions of the ion explicitly within the channel, this number falls to 7 ± 4, as expected from the interference of the serine sidechains with the ion's movement when it is off-axis.

In Fig. 3 we show two-dimensional slices through the full three-dimensional free energy. The slices are separated by 2.0 Å. As stated above, the six-fold symmetry is enforced by the density being replicated (though the *b*-spline contouring of the gridded data used in the graphs obscures this in certain cases). The error in these free energies was estimated by recalculating them from data from the first and second half of the trajectory separately (data not shown). Typically it is about 1–2 kcal mol^{-1}, but in some cases, structures in the free energy of this size are reliably reproduced in the results from the two halves. Only those cases for which this is true are commented upon below.

In a few slices the minimum of free energy lies at the centre of the channel, typically about 1 kcal mol^{-1} deep, though in general the free energy is quite flat across the central region of the channel, of radius ca. 2 Å, corresponding to the HOLE radius. Subsidiary off-axis structures are visible at certain positions, around $z = -7$, -1, $+9$, $+13$ and $+15$ Å (they are visible too at other positions, but in these cases were not reproduced when results from the two halves of the trajectory were compared). At $z = +13$ Å and $+15$ Å, these also seem to correspond to local minima. Around here there is also a local maximum of free energy at the channel centre. However, the existence of off-axis minima does not seem to be strongly correlated with the positions of the serine sidechains, which line the channel fairly uniformly throughout its length. Free energy barriers can clearly be seen around $z = -15$, -3 and $+11$ Å, where the average free energy across the slice increases and the well at the centre of the channel tends to disappear. The free energy is generally higher in the C-terminal (positive z) half of the channel.

The positions of these barriers correlate to some extent with the regions where the channel narrows. This is seen even more clearly in Fig. 4, where we show the one-dimensional free energy profile $F(r)$, where r is the distance from the central pore axis. The apparent central peaks present in these figures do not contradict Fig. 3, because they reflect the increased total probability of finding an ion in an off-axial position, proportional to $2\pi r$, that results when $F(x,y)$ itself is approximately constant. Only in those positions in the C-terminal half of the channel, where F rises very sharply in the middle, is it apparent that a real axis-central maximum has occurred. Further out in the channels, beyond $r = 3$ Å, the free energy increases fairly fast, as the ion is forced into intimate contact with the serine sidechains, though the sidechains are sufficiently flexible, and gaps between them sufficiently accessible, that the energy increases much less rapidly than for a hard-core van der Waals overlap.

This is confirmed by calculations of the coordination of the potassium ion by water or sidechain oxygens. The coordination number is defined as the number of such oxygens closer to the ion than the position of the first minimum of the ion-oxygen radial distribution function in a water box. The total coordination number is about 7.5 in most regions of the channel and water caps, showing a tendency for loss of solvating water to be compensated by serine oxygens as the ion moves off-axis. Nevertheless, when the ion is at $z = +10$ to $+15$ Å, there is a clear reduction in the total degree of hydration to about six oxygens in the first hydration shell, even for the ion in its axial position. There seem to be smaller reductions near $z = 0$ and at the N-terminal mouth too. The average residence time of a water molecule in the ion's first hydration shell before being exchanged also increases from its bulk value of about 12 ps to about

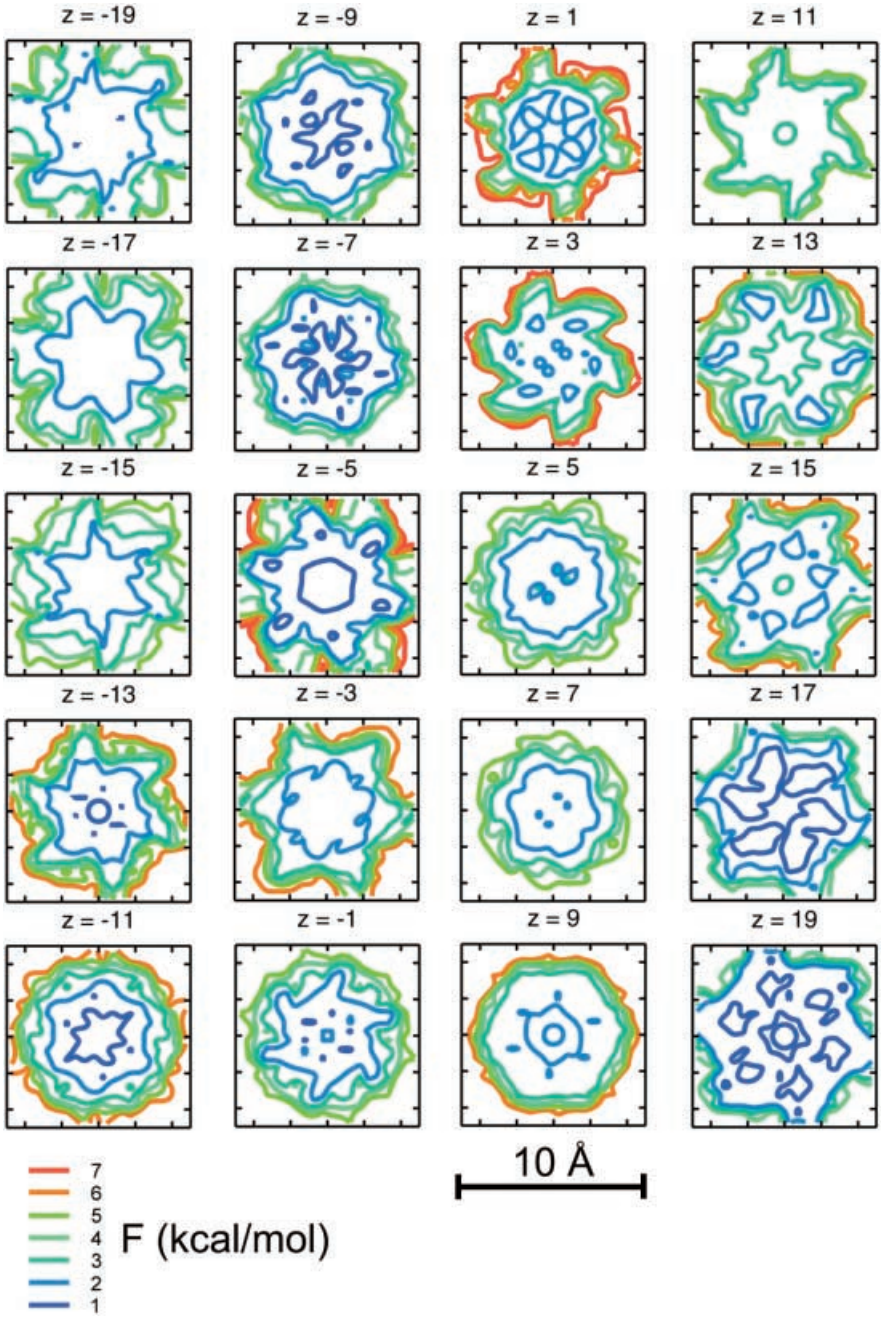

Fig. 3 Contours of free energy in slices perpendicular to the channel axis, for a series of positions along the channel (z) axis (given, in Å, above each panel). In each case the contours are at intervals of 1 kcal mol^{-1}, with the contour levels indicated via the colour scheme given at the bottom of the diagram. Thus, *deep blue* corresponds to the lowest energy contour ($+1$ kcal mol^{-1}) and *red* to the highest ($+7$ kcal mol^{-1})

25 ps. This is similar to the result found by Smith and Sansom (1999).

In Fig. 5 we show the effective $F(z)$ along the length of the channel. The maximum in the C-terminal half of the channel that has already been commented on is clearly visible, along with smaller barriers at the channel centre and the N-terminal mouth. The expected effect of the α-helix dipoles is not visible thoughout the channel, only locally in the barrier near the N-terminal mouth and the reduction at the C-terminal mouth. The local dehydration effects mentioned above seem to be more important in creating free energy barriers.

We can estimate the conductance of the channel from the $F(z)$ curve using the Nernst-Planck equation (Eq. 7). Because we have calculated the free energy of K^+ alone, we must first make the simple approximation that Cl^- ions do not contribute to the current. We have used a spatially varying diffusion coefficient estimated by MD simulations on a very similar LS3 model to the present one in a previous paper (Smith and Sansom 1999), and the channel cross-sectional area A was taken to be 50 Å^2. The results are shown in Fig. 6. For the positive-voltage quadrant, the agreement is quite good. This corresponds to K^+ ions flowing from the N-terminal to the C-terminal mouth of the channel. However, the conductance is underestimated for currents corresponding to K^+ ions flowing in the opposite direction.

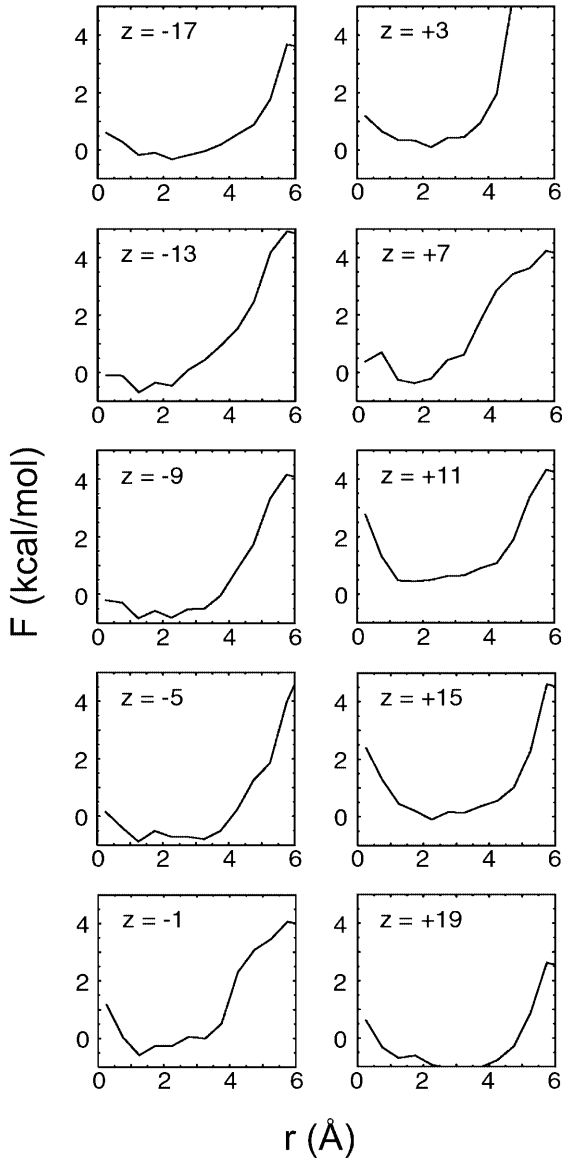

Fig. 4 Free energy as a function of radial position of the ion in the channel, for a series of positions along the channel (z) axis (given, in Å, within each panel)

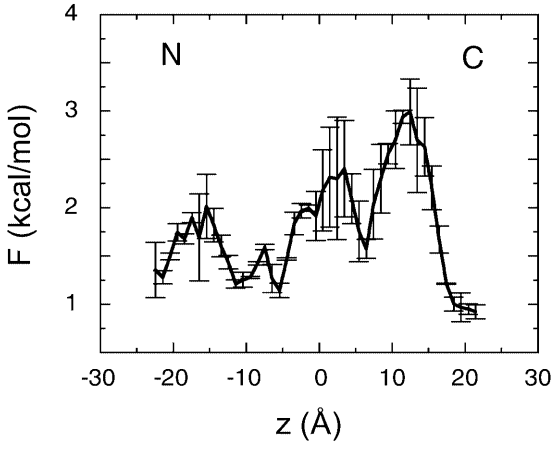

Fig. 5 Free energy $F(z)$ of the potassium ion in the channel as a function of axial position. The *error bars* come from calculating $F(z)$ separately from the first and second halves of each MD trajectory

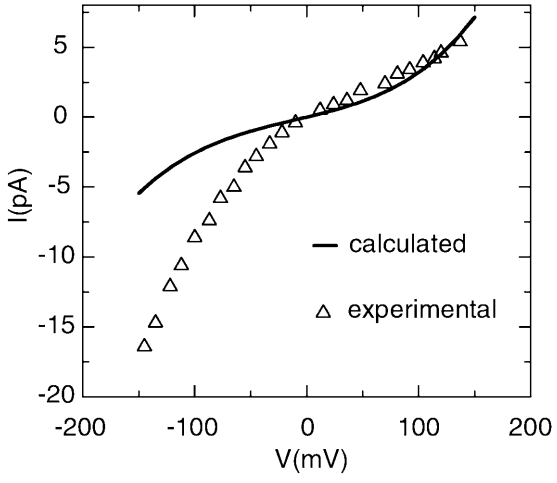

Fig. 6 Predicted and experimental current-voltage relations of the channel, using the free energy profile from Fig. 4 and one-dimensional Nernst-Planck electrodiffusion theory (see text for details). The experimental results are taken from Dieckmann et al. (1999)

Discussion

Although the three-dimensional structure of the LS3 peptide has not been determined at atomic resolution, the channel that it forms is almost certainly an α-helix bundle (Åkerfeldt et al. 1993; Chung et al. 1992; Lear et al. 1994). The peptide was designed precisely so that it would, in that conformation, form amphipathic rods which could then associate in a membrane to form a bundle which would expose hydrophobic leucine residues to the lipid while surrounding an aqueous pore, stabilized by virtue of being lined with hydrophilic serine residues. Since its synthesis (Lear et al. 1988), LS3 has been the subject of extensive studies by electrophysiology (Åkerfeldt et al. 1993; Kienker et al. 1994; Kienker and Lear 1995; Lear et al. 1988), circular dichroism (corroborating the idea that it forms an α-helical bundle) (Lear et al. 1994) and computer simulation (Mitton and Sansom 1996; Randa et al. 1999; Zhong et al. 1998). The exact degree of oligomerization in the channel-forming state is not certain, but a degree of association of six peptides per channel seems the most likely (Mitton and Sansom 1996; Zhong et al. 1998), and is being used here. The LS3 peptide contains no ionizable amino acid residues, for which the ionization state in a membrane environment would be uncertain (and quite possibly dynamically changing during ion passage), or aromatic amino acids, for which the adequacy of present simulation models in treating cation-π-electron interactions is questionable. Moreover, the ion is not forced at any point into very intimate contact with the channel, as it is

in gramicidin or in the selectivity filter of the KcsA channel (Wallace 2000), a situation which once again present force fields have difficulty in treating because of the strong resulting ion-induced dipole interactions. As far as is known, this type of ion permeation is likely to be relevant to channels such as the nicotinic acetylcholine receptor (Unwin 1995, 1996, 2000) or the M2 protein from influenza A (Forrest et al. 1998). LS3 is also thought to be a single-ion channel (i.e. typically occupied by only one ion at a time during conductance) and thus the single-ion free-energy profile obtained is more directly relevant to the permeation process than would be the case for a multi-ion channel like KcsA (Åqvist and Luzhkov 2000; Bernèche and Roux 2001). For these reasons, we consider that the utility of the LS3 channel model as a test-bed for the methods described here outweighs the disadvantage of its unknown structure. The calculations we carry out also incidentally provide a test of the plausibility of the structure, but that is not the main thrust of the work described here.

It is not possible to decompose the free energy as measured above into entropic and enthalpic contributions (using the equation $F = E–TS$). In an MD simulation, the fluctuations of the total internal energy of the system are so large, of the order of 60 kcal mol^{-1}, that E cannot be determined with sufficient precision to detect variations of about the same size as the variation of F that is being investigated. It seems probable that the barriers observed in the channel have both entropic (because the ion has less freedom in x and y) and enthalpic (because of the slightly reduced degree of hydration) components. Similarly, the increase in free energy as the ion comes into contact with the serine sidechains will have both entropic (as the ion and sidechain are reduced in mobility) and enthalpic parts.

Nevertheless, the free energy density that has been determined here does not give particularly good agreement with the experimental single-channel conductance; the agreement in the outward direction is good but the inward current is underestimated. There are several reasons why this might be; for example: (1) the simple 1D free energy profile used in the calculation cannot reproduce effects resulting from the likely off-axis position of the ion as it permeates the C-terminal half of the channel; (2) the simulated system contains only an approximate bilayer mimic, in the form of the restrained methane spheres, and there is no membrane potential; (3) any fluctuations of the system that occur on a longer timescale than the 100 ps of each simulation (e.g. protein conformational changes, movements of ions in the caps) are not taken into account; (4) despite our efforts to avoid it, the restraints applied to the channel may significantly affect the free energy due to perturbation of the channel's natural motions, which may respond to the ion and couple to its transport. Of these effects, (2) may be the largest, due mainly to the missing lipid headgroups. While the accurate calculation of the electrostatic field due to the headgroups would require a Poisson-Boltzmann electrostatics calculation, which we have not carried out, an estimate of the effect from the first couple of layers of lipids around the channel (using Coulomb's law) suggests that they could produce an appreciable perturbation in the ion's free energy, expected to be first an increase in energy, then a decrease, at each channel mouth, with a peak-to-peak height of 1–2 kcal mol^{-1}. However, perhaps the most likely source of the discrepancy in the single channel conductance is the narrower C-terminal half of the LS3 channel compared to the full bilayer simulation, leading to partial dehydration of the ion. In Dieckmann et al. (1999), where a continuum electrostatics approach was used, good agreement with the experimental I-V curve was obtained using an electrostatic energy profile of potassium that is very similar to the free energy calculated here, except that it has a potential well in the C-terminal half of the channel, rather than a barrier. The latter consideration is a more general problem in trying to link atomistic simulations of conformationally mobile channel proteins to calculations of their electrophysiological properties. Free energy profile simulations can address a timescale of ca. 0.1–10 ns. Single ion channel measurements (i.e. I-V curves determinations) are made on a timescale of ca. 0.1–10 ms. Therefore we have a gap of six orders of magnitude. It is likely that a channel may sample many subtly different conformations in ca. 1 ms. Therefore, our simulations may have captured, for example, a sub-conductance level or incompletely open state of the LS3 channel.

In combination with the measurements of diffusion coefficients, the measurement of a free energy profile provides useful input for Brownian dynamics simulations on a reduced representation of an ion channel system (Chung et al. 1999; Im et al. 2000; Phale et al. 2001; Schirmer and Phale 1999), reducing the number of free parameters at present used in these simulations. However, the current simulations suggest that care needs to be paid to the conformational state or states employed in both the free energy calculations and the Brownian dynamics simulations.

The umbrella sampling method used here is one of two methods commonly used to measure free energies, the other being thermodynamic integration (TI). A TI approach was used in the pioneering free energy calculation on gramicidin (Roux and Karplus 1991). Umbrella sampling's advantages lie in the easier estimation of sampling errors, the ability to deal easily and consistently with multi-dimensional free energies, where different possible "paths" though the space connecting the same two point must be taken into account, and in greater efficiency, at least in those cases where the integrand in TI varies rapidly or contains singularities (a common occurrence in simulations where alchemical changes are made).

In summary, we have measured the position-dependent free energy of K^+ in a simple ion channel model and used it to estimate the channel's conductance. Our results show that for this channel, which is lined by hydrophilic sidechains, there is a relatively weak

dependence of the free energy on the axial/off-axial position of the ion. The agreement of the calculated ionic current with experiment is only moderate, most likely as a consequence of problems in more fully sampling the conformational dynamics of the channel. This emphasizes the continuing importance of developing rigorous approaches that enable one to relate short timescale atomistic simulations to longer timescale experimental averages, i.e. the need for more complete integration of MD simulations with more mesoscopic modelling approaches.

Acknowledgements This work was supported by grants from the Wellcome Trust. Additional computer time was provided by the Oxford Supercomputing Centre. Our thanks to Tom Woolf for assistance with the WHAM calculation, and to numerous colleagues for their helpful comments on this work.

References

Adcock C, Smith GR, Sansom MSP (1998) Electrostatics and the selectivity of ligand-gated ion channels. Biophys J 75:1211–1222

Adcock C, Smith GR, Sansom MSP (2000) The nicotinic acetylcholine receptor: from molecular model to single channel conductance. Eur Biophys J 29:29–37

Åkerfeldt KS, Lear JD, Wasserman ZR, Chung LA, DeGrado WF (1993) Synthetic peptides as models for ion channel proteins. Acc Chem Res 26:191–197

Åqvist J, Luzhkov V (2000) Ion permeation mechanism of the potassium channel. Nature 404:881–884

Bernèche S, Roux B (2001) Energetics of ion conduction through the K^+ channel. Nature 414:73–77

Chang G, Spencer RH, Lee AT, Barclay MT, Rees DC (1998) Structure of the MscL homolog from *Mycobacterium tuberculosis*: a gated mechanosensitive ion channel. Science 282:2220–2226

Chen D, Lear J, Eisenberg B (1997) Permeation through an open channel: Poisson-Nernst-Planck theory of a synthetic ionic channel. Biophys J 72:97–116

Chung LA, Lear J, DeGrado WF (1992) Fluorescence studies of the secondary structure and orientation of a model ion channel peptide in phospholipid vesicles. Biochemistry 31:6608–6616

Chung SH, Allen TW, Hoyles M, Kuyucak S (1999) Permeation of ions across the potassium channel: Brownian dynamics studies. Biophys J 77:2517–2533

Dieckmann GR, Lear JD, Zhong Q, Klein ML, DeGrado WF, Sharp KA (1999) Exploration of the structural features defining the conduction properties of a synthetic ion channel. Biophys J 76:618–630

Doyle DA, Cabral JM, Pfuetzner RA, Kuo A, Gulbis JM, Cohen SL, Cahit BT, MacKinnon R (1998) The structure of the potassium channel: molecular basis of K^+ conduction and selectivity. Science 280:69–77

Eisenberg RS (1999) From structure to function in open ionic channels. J Membr Biol 171:1–24

Forrest LR, DeGrado WF, Dieckmann GR, Sansom MSP (1998) Two models of the influenza A M2 channel domain: verification by comparison. Folding Des 3:443–448

Hao Y, Pear MR, Busath DD (1997) Molecular dynamics study of free energy profiles for organic cations in gramicidin A channels. Biophys J 73:1699–1716

Hille B (1992) Ionic channels of excitable membranes, 2nd edn. Sinauer Associates, Sunderland, Mass

Im W, Seefeld S, Roux B (2000) Grand canonical Monte Carlo-Brownian dynamics algorithm for simulating ion channels. Biophys J 79:788–801

Jorgensen WL, Blake JF, Buckner JK (1989) Free energy of TIP4P water and the free-energies of hydration of CH_4 and Cl^- from statistical perturbation theory. Chem Phys 129:193–200

Ketchem RR, Hu W, Cross TA (1993) High-resolution conformation of gramicidin A in a lipid bilayer by solid-state NMR. Science 261:1457–1460

Kienker PK, Lear JD (1995) Charge selectivity of the designed uncharged peptide ion channel Ac-$(LSSLLSL)_3$-$CONH_2$. Biophys J 68:1347–1358

Kienker PK, DeGrado WF, Lear JD (1994) A helical-dipole model describes the single-channel current rectification of an uncharged peptide ion channel. Proc Natl Acad Sci USA 91:4859–4863

Kraulis PJ (1991) MOLSCRIPT: a program to produce both detailed and schematic plots of protein structures. J Appl Crystallogr 24:946–950

Kumar S, Bouzida D, Swendsen RH, Kollman PA, Rosenberg JM (1992) The weighted histogram analysis method for free-energy calculations on biomolecules. 1. The method. J Comput Chem 13:1011–1021

Lear JD, Wasserman ZR, DeGrado WF (1988) Synthetic amphiphilic peptide models for protein ion channels. Science 240:1177–1181

Lear JD, Wasserman ZR, DeGrado WF (1994) Use of synthetic peptides for the study of membrane protein structure. In: White SH (ed) Membrane protein structure: experimental approaches. Oxford University Press, Oxford

Merritt EA, Bacon DJ (1997) Raster3D: photorealistic molecular graphics. Methods Enzymol 277:505–524

Mitton P, Sansom MSP (1996) Molecular dynamics simulations of ion channels formed by bundles of amphipathic α-helical peptides. Eur Biophys J 25:139–150

Miyazawa A, Fujiyoshi Y, Stowell M, Unwin N (1999) Nicotinic acetylcholine receptor at 4.6 angstrom resolution: transverse tunnels in the channel wall. J Mol Biol 288:765–786

Partenskii MB, Jordan PC (1992) Theoretical perspectives on ion-channel electrostatics – continuum and microscopic approaches. Q Rev Biophys 25:477–510

Phale PS, Philippsen A, Widmer C, Phale VP, Rosenbusch JP, Schirmer T (2001) Role of charged residues at the OmpF porin channel constriction probed by mutagenesis and simulation. Biochemistry 40:6319–6325

Randa HS, Forrest LR, Voth GA, Sansom MSP (1999) Molecular dynamics of synthetic leucine-serine ion channels in a phospholipid membrane. Biophys J 77:2400–2410

Roux B (1996) Valence selectivity of the gramicidin channel: a molecular dynamics free energy perturbation study. Biophys J 71:3177–3185

Roux B (1999) Statistical mechanical equilibrium theory of selective ion channels. Biophys J 77:139–153

Roux B, Karplus M (1991) Ion transport in a model gramicidin channel: structure and thermodynamics. Biophys J 59:961–981

Roux B, Bernèche S, Im W (2000) Ion channels, permeation and electrostatics: insight into the function of KcsA. Biochemistry 39:13295–13306

Schirmer T, Phale PS (1999) Brownian dynamics simulation of ion flow through porin channels. J Mol Biol 294:1159–1167

Smart OS, Goodfellow JM, Wallace BA (1993) The pore dimensions of gramicidin A. Biophys J 65:2455–2460

Smith GR, Sansom MSP (1998) Dynamic properties of Na^+ ions in models of ion channels: a molecular dynamics study. Biophys J 75:2767–2782

Smith GR, Sansom MSP (1999) Effective diffusion coefficients of K^+ and Cl^- ions in ion channel models. Biophys Chem 79:129–151

Tieleman DP, Biggin PC, Smith GR, Sansom MSP (2001) Simulation approaches to ion channel structure-function relationships. Q Rev Biophys 34:473–561

Torrie GM, Valleau JP (1977) Nonphysical sampling distributions in Monte-Carlo free energy distributions: umbrella sampling. J Comput Phys 23:187–199

Unwin N (1995) Acetylcholine receptor channel imaged in the open state. Nature 373:37–43

Unwin N (1996) Projection structure of the nicotinic acetylcholine receptor: distinct conformations of the α subunits. J Mol Biol 257:586–596

Unwin N (2000) The Croonian lecture 2000. Nicotinic acetylcholine receptor and the structural basis of fast synaptic transmission. Phil Trans R Soc Lond B 355:1813–1829

Wallace BA (2000) Common structural features in gramicidin and other ion channels. Bioessays 22:227–234

Woolley GA, Biggin PC, Schultz A, Lien L, Jaikaran DCJ, Breed J, Crowhurst K, Sansom MSP (1997) Intrinsic rectification of ion flux in alamethicin channels: studies with an alamethicin dimer. Biophys J 73:770–778

Zhong Q, Moore PB, Newns DM, Klein ML (1998) Molecular dynamics study of the LS3 voltage-gated ion channel. FEBS Lett 427:267–270